

Supporting Information for "Long-term Surface Temperature (LoST) Database as a complement for GCM preindustrial simulations"

Francisco José Cuesta-Valero^{1,2}, Almudena García-García^{1,2}, Hugo Beltrami², Eduardo Zorita³, and Fernando Jaume-Santero^{2,4}

¹Environmental Sciences Program, Memorial University of Newfoundland, St. John's, NL, Canada.

²Climate & Atmospheric Sciences Institute, St. Francis Xavier University, Antigonish, NS, Canada.

³Institute of Coastal Research, Helmholtz-Zentrum Geesthacht, Germany.

⁴Departamento de Física de la Tierra y Astrofísica, Facultad de Ciencias Físicas, Universidad Complutense de Madrid, 28040, Madrid, Spain.

S1 Error Propagation for LoST Database

The GIDS algorithm (Eq. 3) incorporates errors from the determination of the latitudinal, longitudinal and altitudinal gradients as well as errors from the T_0 estimates. Errors in T_0 temperatures are specified by the linear regression analysis employed to determine the T_0 values from each BTP measurement, while the linear regression analysis of the geographical distribution of T_0 temperatures provides the latitudinal, longitudinal and altitudinal gradients and their errors (see Section 3). Therefore, an estimate of the error in LoST temperatures at each grid cell of the database can be computed just by applying basic error propagation theory to Eq. 3, which results in:

$$\Delta V_0 = \frac{\sqrt{\sum_{i=1}^N \left\{ \left(\Delta V_i^2 + (|lat_0 - lat_i| \Delta C_{lat})^2 + (|lon_0 - lon_i| \Delta C_{lon})^2 + (|z_0 - z_i| \Delta C_z)^2 \right)^{\frac{1}{2}} |d_i^{-2}| \right\}^2}}{\left| \sum_{i=1}^N d_i^{-1} \right|} \quad (S1)$$

where ΔV_0 is the error of the predicted temperature at the target node, ΔV_i represents the T_0 error from the i^{th} BTP measurement, ΔC_{lat} , ΔC_{lon} and ΔC_z are the errors in the gradients from the regression analysis of the geographical distribution of T_0 data, lat_i , lon_i and z_i represent latitude, longitude and altitude of the i^{th} measurement respectively, lat_0 , lon_0 and z_0 represent the latitude, longitude and altitude of the target node respectively, d_i is the distance from the i^{th} measurement to the target node, and N are the number of BTP measurements within a distance of 650 km to the target node. Errors in latitude, longitude and altitude are considered negligible, as well as the error in the distance between measurements and target nodes. Fig. S6 shows the errors as 2σ values (i.e., $2 \times \Delta V_0$) for each grid cell, with a spatial average of $0.2 \text{ }^\circ\text{C}$.

Beyond the propagation of known errors, other sources of error are possible but difficult to characterize given the limited temporal resolution of the LoST database. The most probable additional source of error is the distance criterion for the interpolation. This criterion was determined using a pseudo-proxy experiment and five PMIP3/CMIP5 PM simulations, obtaining

different results for each model (Fig. S1). However, we did not find any adequate method to characterize such error in the LoST database, and further sources of error are possible.

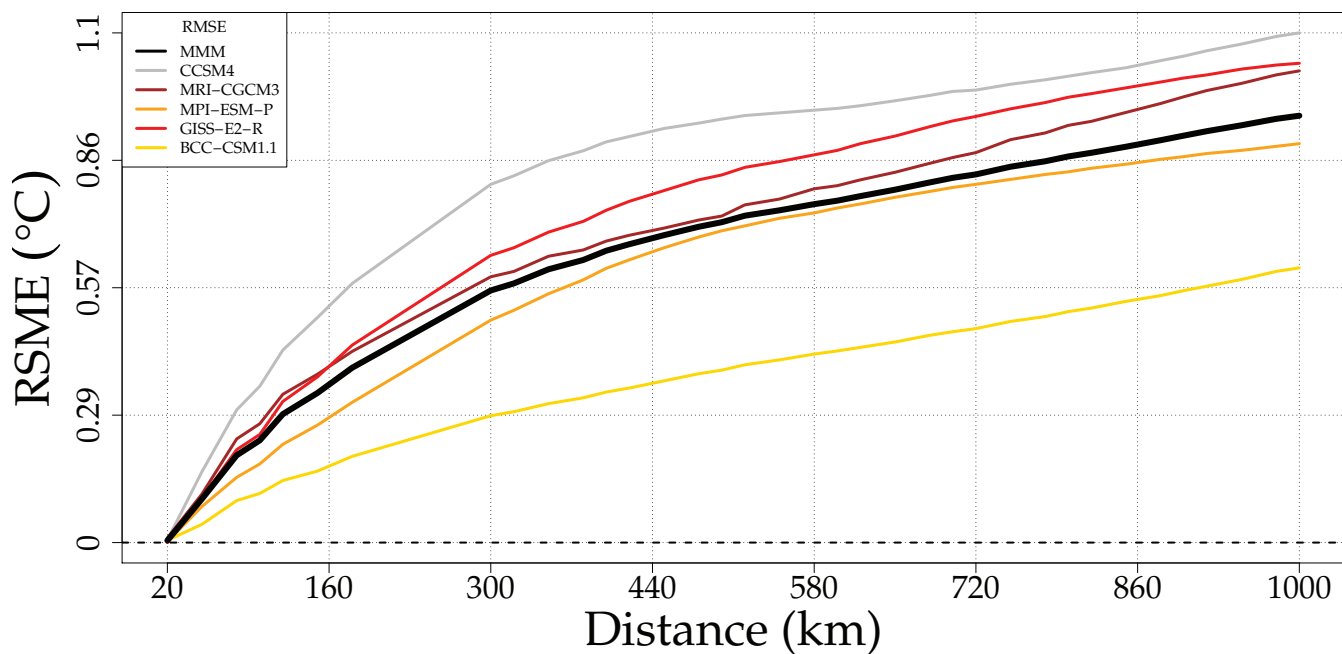


Figure S1. Root-Mean Squared Errors of the GIDS interpolation using ground surface temperatures at 1.0 m depth for the period 1300-1700 CE from the PMIP3/CMIP5 PM simulations to obtain a maximum distance criterion to interpolate each BTP measurement. The black line represents the multimodel mean (MMM).

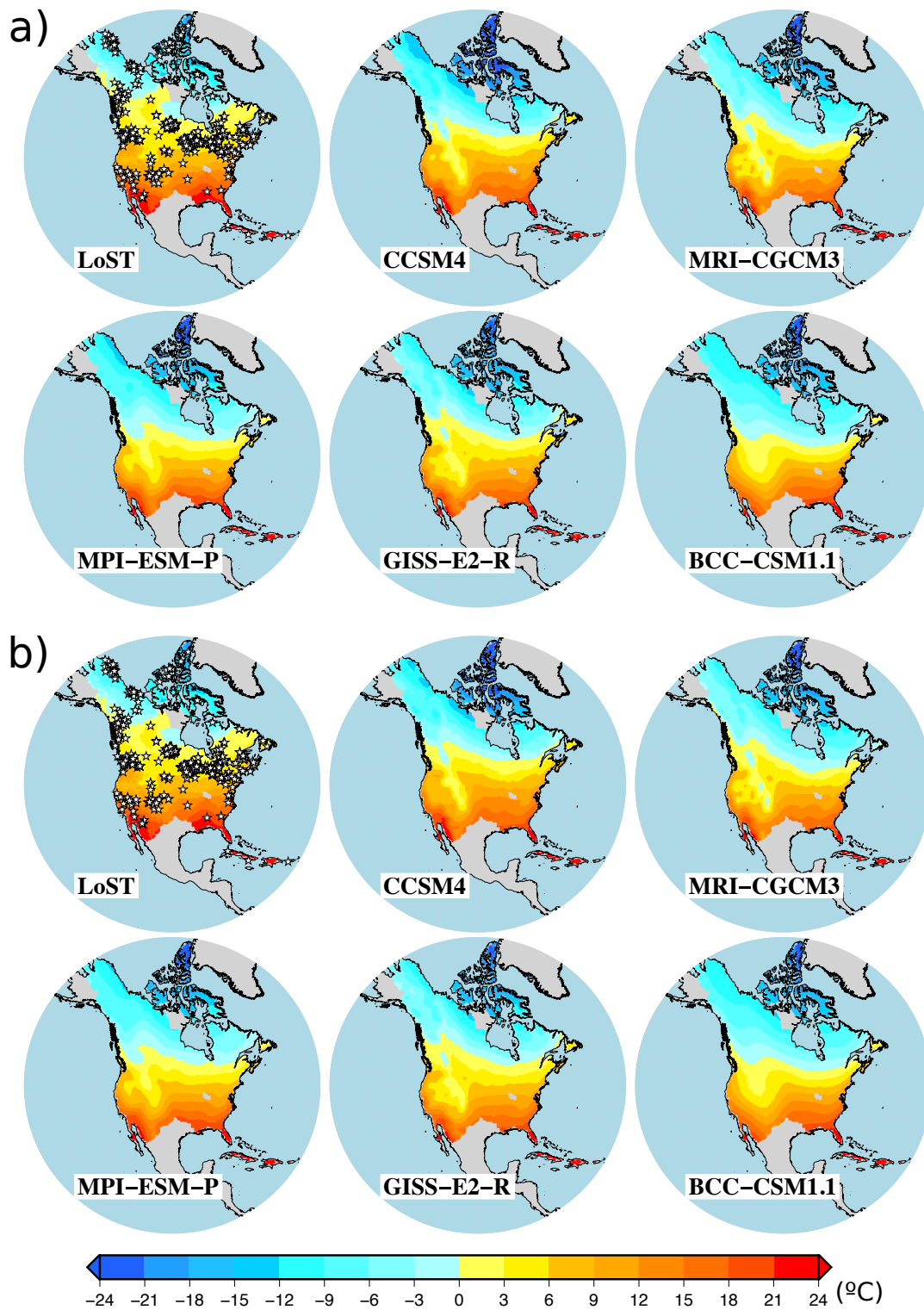


Figure S2. SAT_0 estimates from (a) PMIP3/CMIP5 PM simulations (1300-1700 CE) and (b) PMIP3/CMIP5 piControl simulations together with LoST temperatures. White stars show the location of the employed BTP measurements for the GIDS interpolation.

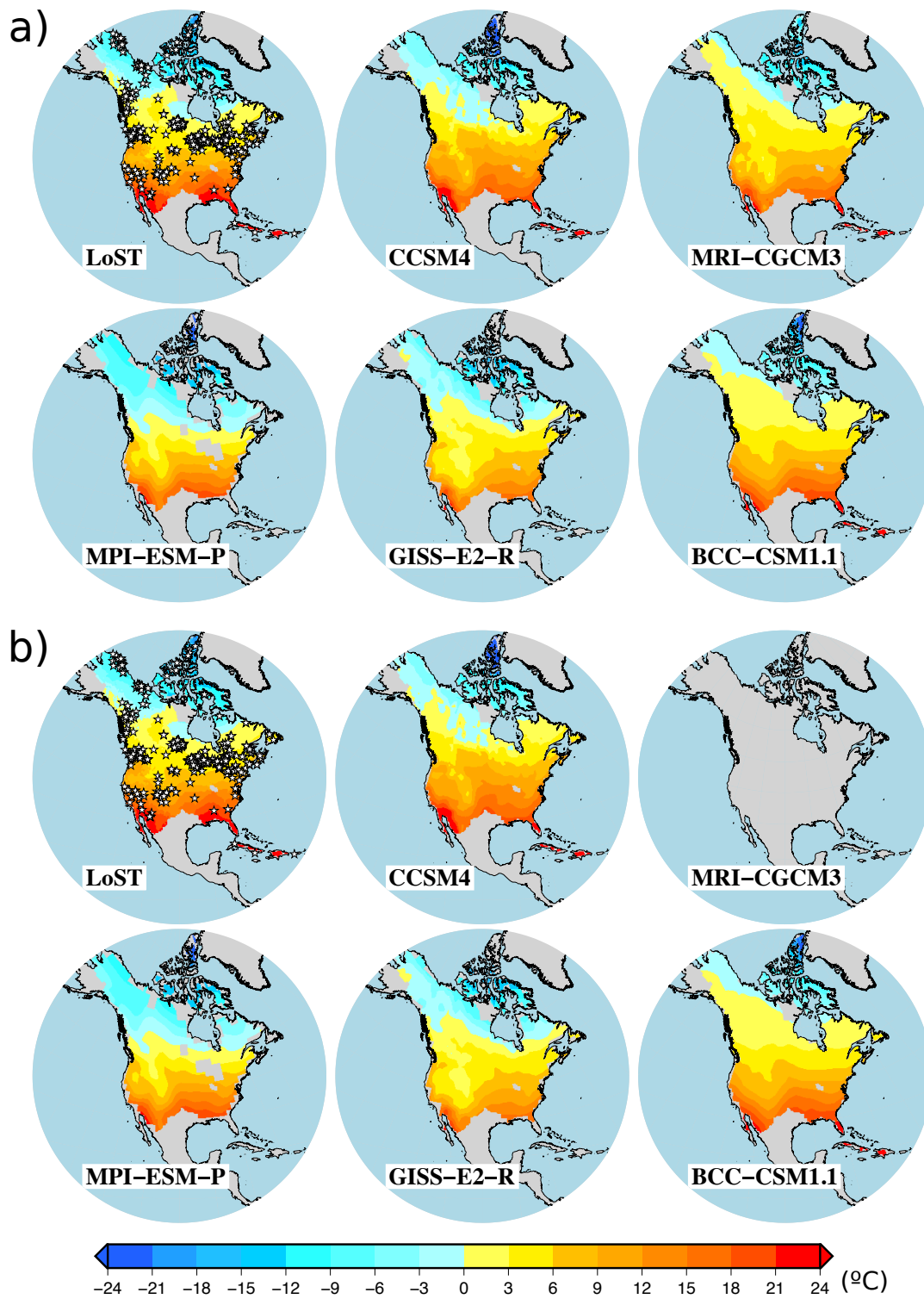


Figure S3. GST_0 estimates from (a) PMIP3/CMIP5 PM simulations (1300-1700 CE) and (b) PMIP3/CMIP5 piControl simulations together with T_0 temperatures. White stars shown the location of the employed BTP measurements for the GIDS interpolation.

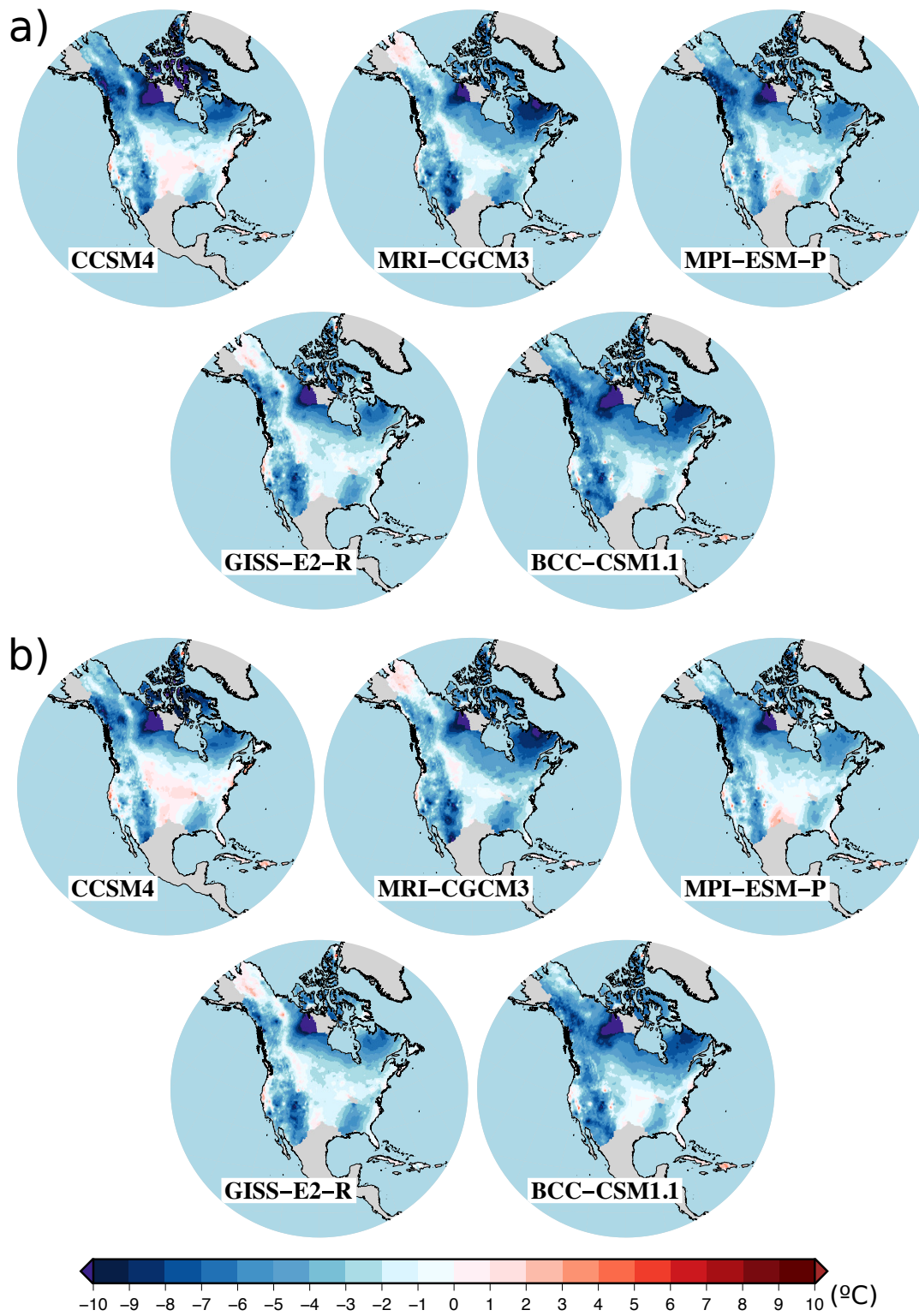


Figure S4. Difference between SAT_0 values from PMIP3/CMIP5 simulations and LoST temperatures. (a) Results for PM simulations (1300-1700 CE). (b) Results piControl simulations.

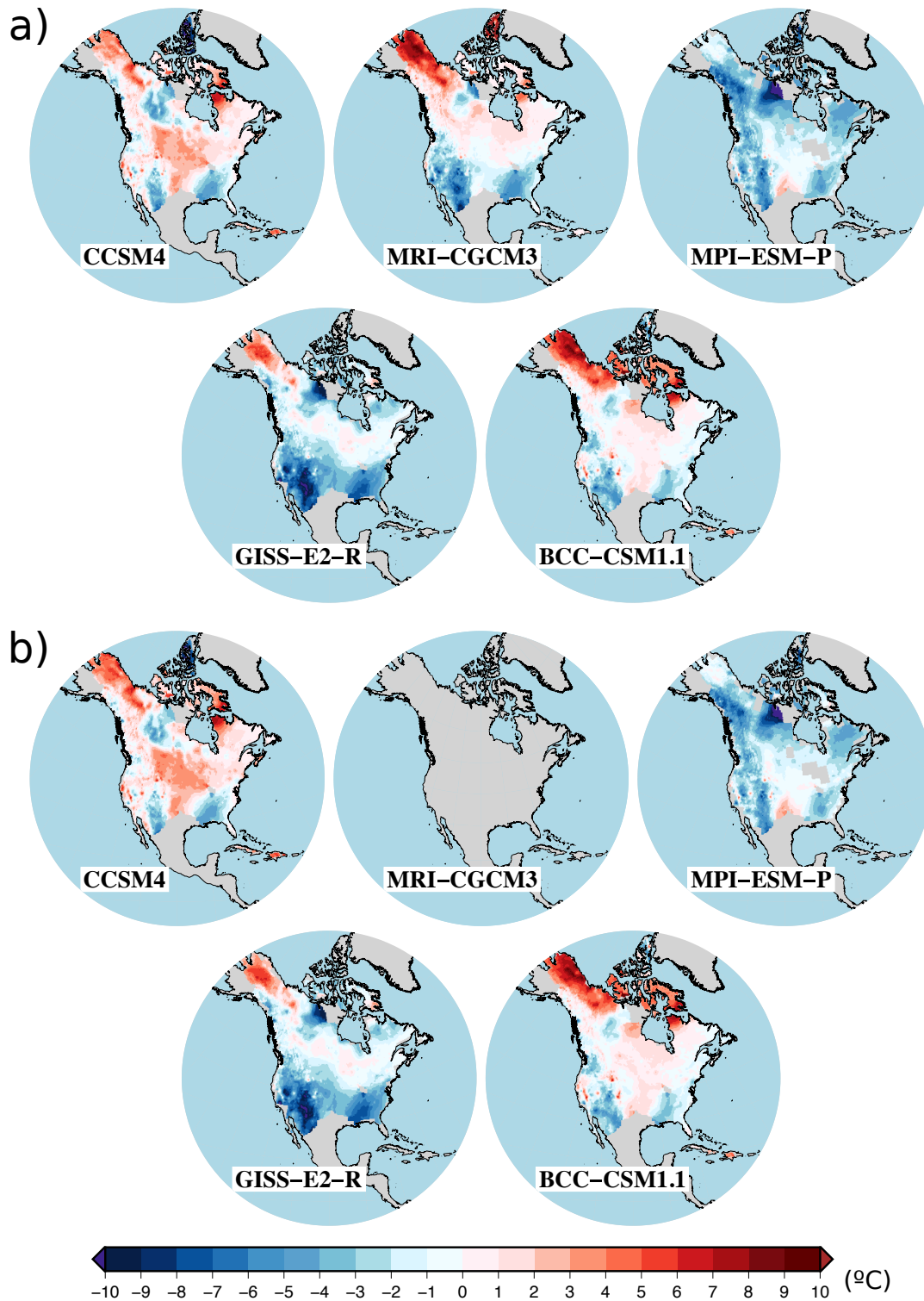


Figure S5. Difference between GST_0 values from PMIP3/CMIP5 simulations and LoST temperatures. (a) Results for PM simulations (1300-1700 CE). (b) Results for piControl simulations.

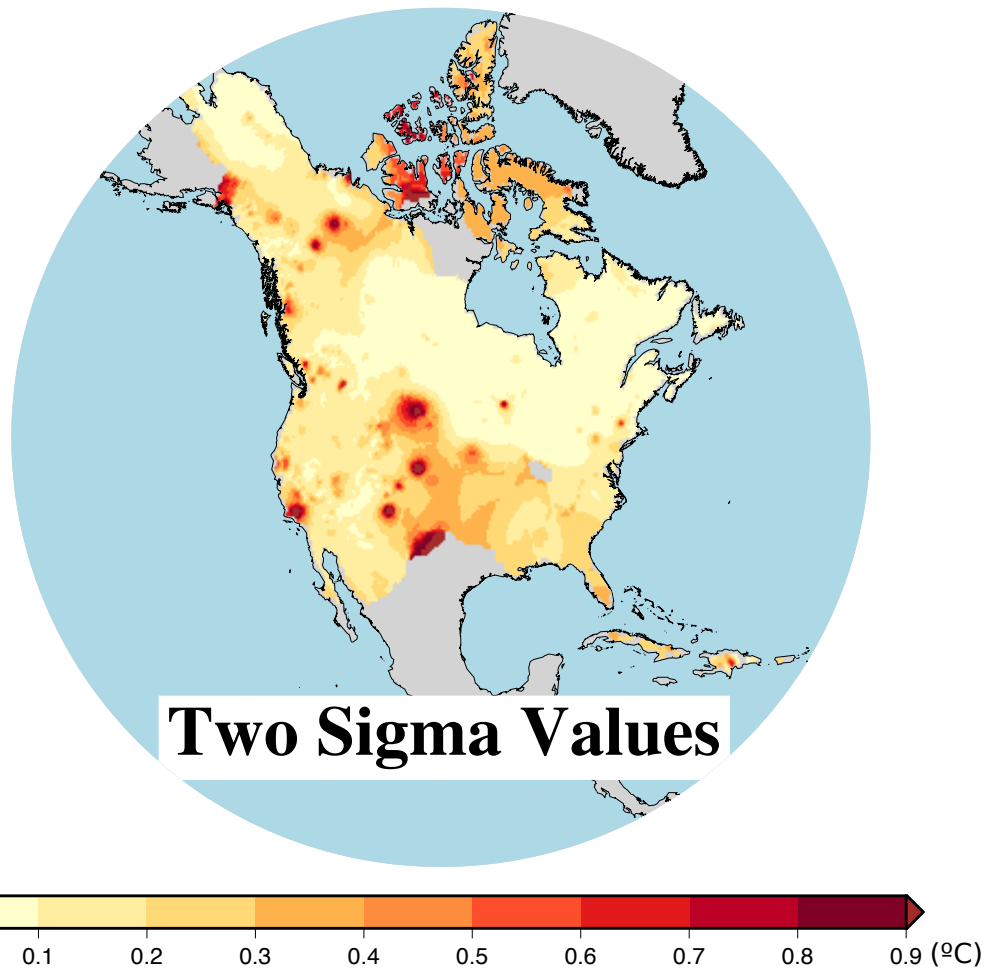


Figure S6. Errors (2σ values) of LoST temperatures estimated as described in Section S1. The spatial average is $0.2\text{ }^{\circ}\text{C}$.

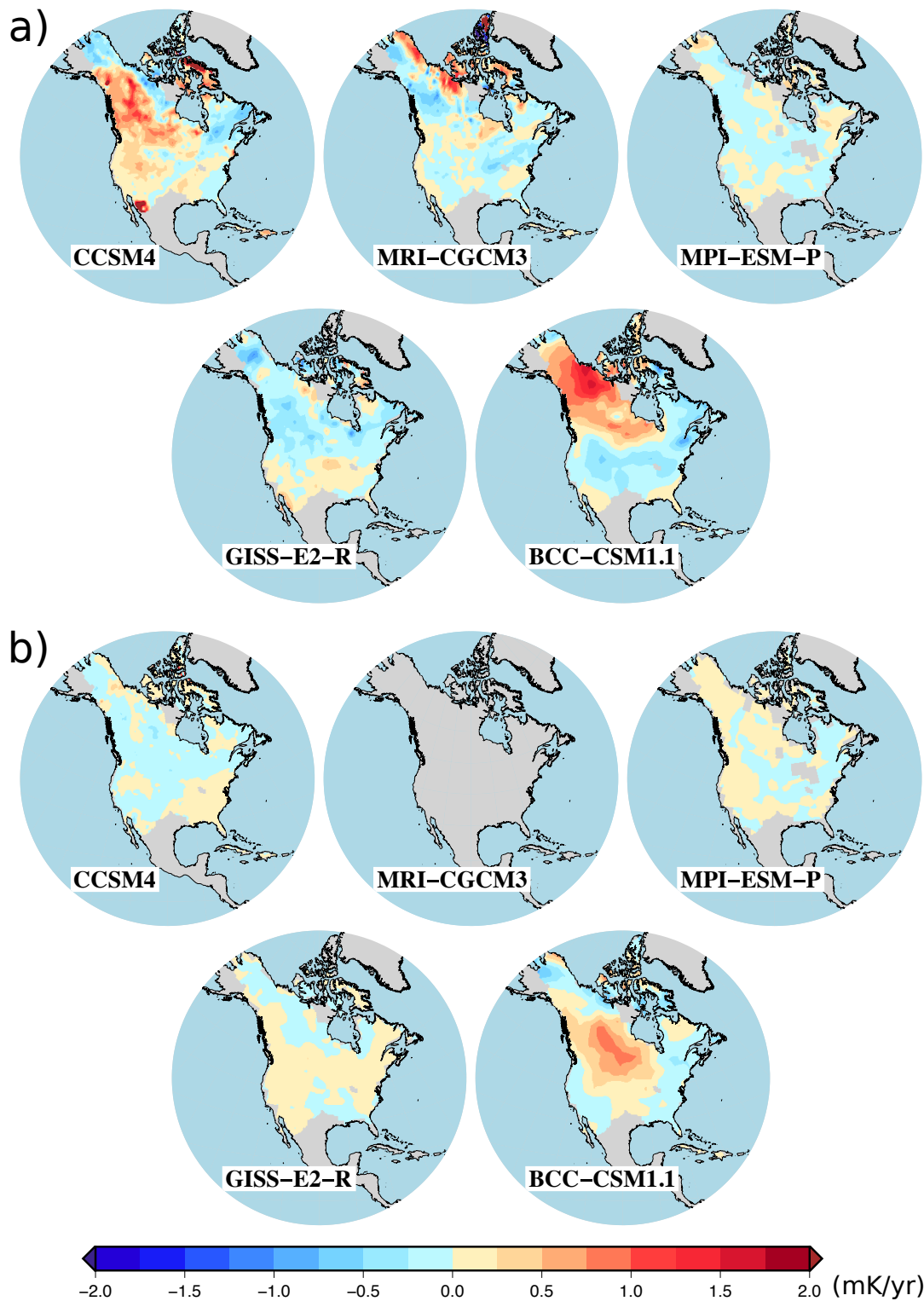


Figure S7. Trends of the difference between air and ground (1.0 m depth) temperatures from PMIP3/CMIP5 simulations. (a) Results for PMIP simulations (1300-1700 CE). (b) Results for piControl simulations. 9